International Research Journal on Advanced Engineering and Management
https://goldncloudpublications.com
https://doi.org/10.47392/IRJAEM.2025.0385
e ISSN: 2584-2854
Volume: 03
Issue:07 July 2025
Page No: 2441 - 2450

Influence of Thermal Environment on the Parametric Instability of a Sinusoidally Tapered Rotating Sandwich Beam

Madhusmita Pradhan[1], Nabakishor Dang[2], Manabhanjan Panda[3], Prasanta Kumar Pradhan[4], Pusparaj Dash[5], Madhumita Mohanty[6]

[1]Assistant professor, Dept. of ME, VSSUT., Burla, Odisha, India.

[2, 3]Ph.d Scholar, Dept. of ME, VSSUT., Burla, Odisha, India.

[4]Associate professor, Dept. of ME, VSSUT., Burla, Odisha, India.

[5]Professor, Dept. of ME, VSSUT., Burla, Odisha, India.

[6]Assistant professor, Dept. of ME, KIIT-DU., Bhubaneswar, Odisha, India.

Email ID: *osme.madhusmita@gmail.com[1], nabakishordang@gmail.com[2], manabhanjanpanda956@gmail.com[3], prasant2001uce@gmail.com[4], prdash_india@yahoo.co.in[5], madhumita.mohanty92@gmail.com[6]*

Abstract

This study investigates the dynamic stability of rotating sandwich beams featuring a sinusoidal taper profile under combined periodic axial loading and thermal gradients. Using the extended Hamilton's principle, we derive the governing equations that account for shear deformation, rotary inertia, and the unique stiffness distribution created by the sinusoidal thickness variation. The resulting equations are transformed into non-dimensional form and solved using the extended Galerkin method, with parametric instability regions identified through the Saito-Otomi criteria. Our analysis reveals that the amplitude and phase characteristics of the sinusoidal taper significantly influence the stability boundaries, with optimal tapering parameters demonstrating improved vibration suppression compared to traditional uniform, parabolic and linear profiles. The results demonstrate complex interactions between rotational effects, thermal gradient, shear parameter, core-loss factor and taper geometry, showing that moderate sinusoidal tapering combined with high rotational speeds can substantially enhance stability, while thermal gradients tend to reduce the stable operating regions. These findings provide valuable insights for the design of advanced rotating structures in aerospace and energy applications where dynamic stability and weight optimization are critical.

Keywords: *Sandwich beam, Axial pulsating load, Dynamic stability, Thermal gradient, sinusoidal Taper Parameter.*

1. Introduction

Sinusoidally tapered sandwich beams offer significant advantages in aerospace, automotive, and civil engineering applications where weight reduction, vibration suppression, and optimized load distribution are critical. The sinusoidal taper profile provides a smooth stiffness transition along the beam length, minimizing stress concentrations and improving dynamic stability compared to conventional linear or parabolic tapers. In aerospace structures, such as helicopter rotor blades and aircraft wings, this design enhances aeroelastic performance by reducing flutter susceptibility while maintaining structural integrity under cyclic loading. For automotive suspension systems, the sinusoidal taper helps dampen vibrations and absorb impact energy more efficiently. Additionally, in civil engineering, these beams can be employed in long-span bridges and high-rise buildings to mitigate wind-induced oscillations and seismic effects. The sandwich construction—with a lightweight core and high-

International Research Journal on Advanced Engineering and Management
https://goldncloudpublications.com
https://doi.org/10.47392/IRJAEM.2025.0385
e ISSN: 2584-2854
Volume: 03
Issue:07 July 2025
Page No: 2441 - 2450

strength face sheets—further enhances strength-to-weight ratios, making sinusoidally tapered sandwich beams ideal for applications requiring both durability and energy efficiency. This study explores their dynamic stability under rotational and thermal loads, providing insights for next-generation structural designs.The phenomenon of parametric excitation was first systematically observed by Faraday [1], who discovered that a fluid's free surface oscillates at half the excitation frequency when its container undergoes vertical vibrations. This fundamental finding laid the groundwork for subsequent investigations into the dynamic behavior of elastic structures. Hetenyi's pioneering work [2] on beams supported by elastic foundations established critical theoretical frameworks that remain relevant across multiple engineering disciplines. Recent studies have significantly advanced our understanding of tapered and composite beam systems. Pradhan [3] examined the stability characteristics of irregularly tapered sandwich beams on Pasternak foundations under pulsating loads, while Yokoyama [4] employed finite element analysis to study Timoshenko beams on elastic substrates. Several researchers, including Ding et al. [5] and Lenci and Clementi [6], have contributed valuable insights into nonlinear foundation behavior and layered beam dynamics through various analytical and computational approaches. The thermo-mechanical stability of advanced composite structures has received particular attention in contemporary research. Pradhan and Murmu [7] investigated functionally graded sandwich beams, demonstrating how material gradation influences vibrational characteristics. Subsequent studies by Lenci et al. [8] and Behera [9] expanded this work to include rotating systems and nonlinear oscillations under different boundary conditions. The development of computational methods has enabled more sophisticated analyses, as evidenced by Pradhan and Dash's [10] work on three-layer viscoelastic systems. Foundational studies on beam-foundation interaction [11-16] have been complemented by investigations into constrained-layer damping [20], nonlinear vibrations [22], and parametric stability [23]. Recent advances in material science have introduced new possibilities through functionally graded materials [39-41], while improved computational techniques have enhanced our ability to predict stability boundaries [42]. However, gaps remain in understanding the dynamic behavior of sinusoidally tapered rotating beams under combined thermo-mechanical loading - an area this study seeks to address through comprehensive analytical and numerical investigation. While extensive studies have been conducted on the dynamic stability of sandwich beams with uniform, linear, or parabolic taper profiles under mechanical and thermal loads, the behavior of sinusoidally tapered sandwich beams subjected to combined rotational motion and periodic axial forces remains insufficiently explored. Existing literature primarily focuses on static or simple harmonic loading conditions, often neglecting the complex interaction between time-dependent stiffness variations (induced by sinusoidal tapering) and parametric excitation in rotating systems. Furthermore, most stability analyses employ conventional taper models, overlooking how phase shifts and amplitude modulation in sinusoidal profiles influence instability boundaries. There is also a lack of comprehensive studies examining the synergistic effects of thermal gradients, shear deformation, and rotational speed on such non-uniform structures. This research gap limits the optimization of advanced engineering applications—such as turbomachinery blades and aerospace components—where sinusoidal tapering could offer superior vibration control and weight efficiency. The present work addresses these limitations by developing a generalized analytical framework for sinusoidally tapered rotating sandwich beams, incorporating thermo-mechanical coupling and foundation interaction to enable more accurate stability predictions.

2. Problem Formulation

This study investigates the dynamic response of a rotating sandwich beam featuring an asymmetric sinusoidal taper along its length, subjected to a time-varying axial load. As illustrated in Figure 1, the beam, with total length is mounted eccentrically with respect to the axis of rotation and spins about the vertical axis at a specified angular velocity, A harmonically varying axial force is applied at the

International Research Journal on Advanced Engineering and Management
https://goldncloudpublications.com
https://doi.org/10.47392/IRJAEM.2025.0385
e ISSN: 2584-2854
Volume: 03
Issue:07 July 2025
Page No: 2441 - 2450

beam's free end, aligned with the centroid of the cross-section. This axial excitation comprises both constant (static) and time-dependent (dynamic) components, each defined by their respective amplitude and frequency. The sinusoidal taper introduces a smooth, periodic variation in the beam's cross-sectional geometry, which significantly influences the spatial distribution of stiffness and inertia, and thereby alters the system's dynamic stability under combined mechanical and thermal loading conditions. (Figure 1)

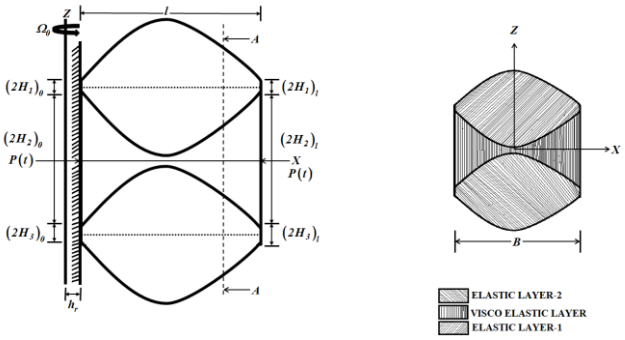

Figure 1 System Configuration

2.1. Notation Used

Table 1 Notation Used

A_{11}, A_{22}, A_{33}	:	Cross-sectional area.
B	:	The beam's width.
E_{11}, E_{33},	:	Young's modulus of elastic layers.
h_r	:	Hub radius.
$2H_1, 2H_2, 2H_3$	:	Depth of 3 layers.
α_{11}, α_{33}	:	Upper and lower-layer taper parameters, respectively.
l	:	Beam length.
Ω_0	:	About z-axis beam's rotational speed.
δ_{11}, δ_{22}	:	Temperature gradients

2.2. Numerical Modelling

The following are the formulas for potential energy, kinetic energy

$$V_v = \frac{1}{2}\int_0^l E_{11,x}A_{11,x}U_{1,x}^2 dx + \frac{1}{2}\int_0^l E_{33,x}A_{33,x}U_{3,x}^2 dx + \frac{1}{2}\int_0^l \left(E_{11,x}I_{1,x} + E_{33,x}I_{3,x}\right)w_{,xx}^2 dx + \frac{1}{2}G_2^*\int_0^l A_{22,x}\gamma_2^2 dx \quad (01)$$

$$T_t = \frac{1}{2}\int_0^l \bar{m}_T w_{,t}^2 dx + \frac{1}{2}\int_0^l \bar{m}_T \Omega_0^2 w^2 dx + \frac{1}{2}\Omega_0^2\int_0^l \left[\bar{m}_T\left(h_r + x\right)\int_0^x w_{,x}^2\, dx\right]dx \quad (02)$$

$$W_w = \frac{1}{2}\int_0^l P(t)\, w_{,x}{}^2\, dx \quad (03)$$

Work done is

U_1, U_2 Are the elastic layer's axial displacements, where for the middle layer's shear strain $w_{,x} = \frac{\partial w}{\partial x}, w_{,t} = \frac{\partial w}{\partial t}, \gamma_2$ are taken, for $\gamma_2 = \frac{U_1 - U_3}{2H_2} - \frac{Cw_{,x}}{2H_2}$ as per Kerwin's assumption [20], U_3 is eliminated.

The sinusoidal taper parameter of the beam is $\left(H_i\right)_x = \left(H_i\right)_0\left\{1 - \alpha_{ii}\, sin^2\left(\frac{\pi x}{l}\right)\right\}$ for $(i = 1,3)$

Where α_i =taper parameters of elastic layers; and $\left(H_i\right)_0$ =height of different layers at the root.

sinusoidal tapper parameter of the upper and bottom layers are, $\alpha_{11} = \frac{H_{10} - H_{1l}}{H_{10}};\ \alpha_{33} = \frac{H_{30} - H_{3l}}{H_{30}}$.

The modulus of elasticity variation for beam $E_{ii}(\bar{x}) = E_{ii0}\left\{1 - \delta_{iix}\, sin^2(\pi\bar{x})\right\}$, for $(i = 1,3)$ (04)

By putting Hamilton's idea into practice,

$$\delta\delta\int_{t_1}^{t_2}\left(T_t - V_v + W_w\right)dt = 0 \quad (05)$$

International Research Journal on Advanced Engineering and Management
https://goldncloudpublications.com
https://doi.org/10.47392/IRJAEM.2025.0385
e ISSN: 2584-2854
Volume: 03
Issue:07 July 2025
Page No: 2441 - 2450

Following are the non-dimensional equation of motions of the system,

$$\left[1+\frac{\lambda_0^2\left(1+E_{31}H_{31}^3\right)}{\left(lH_{10}\right)^2\left(1+E_{31}H_{31}\right)}\left\{\frac{ff}{l^2}-\left(\bar{x}+\bar{h}_r\right)^2\right\}\right]\bar{w}_{,\bar{x}\bar{x}\bar{x}}$$

$$-\frac{2\lambda_0^2\left(1+E_{31}H_{31}^3\right)}{\left(lH_{10}\right)^2\left(1+E_{31}H_{31}\right)}\left(\bar{x}+\bar{h}_r\right)\bar{w}_{,\bar{x}\bar{x}}=0$$

$$\bar{m}_T\bar{w}_{,\bar{t}\bar{t}}+\left[1+\frac{\lambda_0^2\left(1+E_{31}H_{31}^3\right)}{\left(lH_{10}\right)^2\left(1+E_{31}H_{31}\right)}\left\{\frac{ff}{l^2}-\left(\bar{x}+\bar{h}_r\right)^2\right\}\right]\bar{w}_{,\bar{x}\bar{x}\bar{x}\bar{x}}$$

$$-\frac{2\lambda_0^2\left(1+E_{31}H_{31}^3\right)}{\left(lH_{10}\right)^2\left(1+E_{31}H_{31}\right)}\left(\bar{x}+\bar{h}_r\right)\bar{w}_{,\bar{x}\bar{x}\bar{x}}$$

$$+\begin{bmatrix}-\dfrac{\lambda_0^2\left(1+E_{31}h_{31}^3\right)}{\left(lH_{10}\right)^2\left(1+E_{31}H_{31}\right)}\\ -\lambda_0^2\left\{\dfrac{ff}{l^2}-\left(\bar{x}+\bar{h}_r\right)^2\right\}\\ -3g^*\left(1+\dfrac{H_{12}+H_{32}}{2}\right)^2+\bar{P}\left(\bar{t}\right)\end{bmatrix}\bar{w}_{,\bar{x}\bar{x}}$$

$$+\lambda_0^2\left(\bar{x}+\bar{h}_r\right)\bar{w}_{,\bar{x}}+\frac{3}{2}g^*lH_{10}H_{12}\left(1+\frac{H_{12}+H_{32}}{2}\right)$$

$$\left(1+\alpha\right)\frac{2\left(H_2\right)_0}{CC}\gamma_{2,\bar{x}}=0 \quad (06)$$

$$\frac{2\left(H_2\right)_0}{CC}\gamma_{2,\bar{x}\bar{x}}-\frac{g^*}{4}H_{12}^2\left(\frac{1+E_{31}H_{31}^3}{1+\alpha^2E_{31}h_{31}}\right)\left(1+\alpha\right)$$

$$\begin{bmatrix}\left(1+\alpha\right)\dfrac{2\left(H_2\right)_0}{CC}\gamma_2-\\ \left(\dfrac{2\left(1+\left(\left(H_{12}+H_{32}\right)/2\right)\right)}{\left(lH_{10}H_{12}\right)}\right)\bar{w}_{,\bar{x}}\end{bmatrix}=0 \quad (07)$$

$$\bar{m}_T=\left(1+\alpha x\right)\begin{bmatrix}1-\left(\dfrac{\rho_2}{\rho_1}\right)\left(\dfrac{1}{\left(2H_1\right)_0}\right)\\ \left\{\left(2H_2\right)_0+\left(H_1\right)_x+\left(H_3\right)_x\right\}+\\ \left(\dfrac{\rho_3}{\rho_1}\right)\left(\dfrac{\left(H_3\right)_x}{\left(H_1\right)_0}\right)\end{bmatrix} \quad (08)$$

At and, $\bar{x}=0,\bar{x}=1$ are the relevant boundary conditions.

(09)

or, $\bar{w}_{,\bar{x}}=0$ (10)

$$\begin{bmatrix}\dfrac{\lambda_0^2\left(1+E_{31}H_{31}^3\right)}{\left(lH_{10}\right)^2\left(1+E_{31}H_{31}\right)}-\lambda_0^2\left\{\dfrac{ff}{l^2}-\left(\bar{x}+\bar{h}_r\right)^2\right\}-\\ 3g^*\left(1+\dfrac{H_{12}+H_{32}}{2}\right)^2+\bar{P}\left(\bar{t}\right)\end{bmatrix}\bar{w}_{,\bar{x}}=0 \quad (11)$$

or, $\bar{w}=0$ (12)

$$\frac{3}{2}g^*lH_{10}H_{12}\left(1+\frac{H_{12}+H_{32}}{2}\right)$$

$$\left(1+\alpha\right)\frac{2\left(H_2\right)_0}{CC}\gamma_{2,\bar{x}}=0 \quad (13)$$

or, $\gamma_2=0$ (14)

2.3. Solution by Variation Method

Equations (4) and (5) are assumed to have solutions

$$\bar{w}\left(\bar{x},\bar{t}\right)=\sum_{i=1}^{i=P}w_i\left(\bar{x}\right)ff_i\left(\bar{t}\right) \quad (14)$$

$$\bar{\gamma}_2\left(\bar{x},\bar{t}\right)=\sum_{k=P+1}^{k=2P}\gamma_{2k}\left(\bar{x}\right) \quad (15)$$

The shape functions are w_i and γ_{2k} the generalized coordinates are ff_i and ff_k.To satisfy many boundary condition of the system w_i and γ_{2k} are chosen referring from [31].

By utilizing the general Galerkin's approach and substituting the previously given equations in equations (4) and (5).

In addition, in subsequent simulations, five-term approximations are employed for a sequence of solutions

$$[m]\left\{\ddot{Q}_{11}\right\}+[K_{11}]\{Q_{11}\}+[K_{12}]\{Q_{22}\}=\{0\} \quad (16)$$

$$[K_{21}]\{Q_{11}\}+[K_{22}]\{Q_{22}\}=\{0\} \quad (17)$$

Where,

$$\{Q_{11}\}=\left\{ff_1,\ldots\ldots\ldots\ldots,ff_p\right\}^T$$

$$\{Q_{22}\}=\left\{ff_{p+1},\ldots\ldots\ldots\ldots,ff_{2p}\right\}^T$$

International Research Journal on Advanced Engineering and Management
https://goldncloudpublications.com
https://doi.org/10.47392/IRJAEM.2025.0385
e ISSN: 2584-2854
Volume: 03
Issue:07 July 2025
Page No: 2441 - 2450

$$m_{ij} = \int_0^1 \bar{m} w_i w_j d\bar{x} \quad (18)$$

$$K_{11ij} = \int_0^1 \left[1 + \lambda_1 \left\{ \frac{ff}{l^2} - \left(\bar{x} + \bar{h}_r\right)^2 \right\}\right] w_i'' w_j'' d\bar{x} + \lambda_0^2 \int_0^1 \left\{ \frac{ff}{l^2} - \left(\bar{x} + \bar{h}_r\right)^2 \right\} w_i' w_j' d\bar{x} + \begin{Bmatrix} 3g^* \left(1 + \frac{H_{12} + H_{32}}{2}\right)^2 \\ -\bar{P}(\bar{t}) \end{Bmatrix} \int_0^1 w_i' w_j' d\bar{x} \quad (19)$$

$$K_{12jl} = -\left(\frac{3}{2}\right) g^* l H_{10} H_{12} (1+\alpha) \left(1 + \frac{H_{12} + H_{32}}{2}\right) \left(\int_0^1 u_l w_i' d\bar{x} \right) \quad (20)$$

$$K_{22kl} = 3 \times (lH_{10})^2 \frac{\left(1 + \alpha^2 E_{31} H_{31}\right)}{\left(1 + E_{31} H_{31}^3\right)} \left(\int_0^1 u_k' u_l' d\bar{x} \right) + \frac{3}{4} g^* (lH_{10})^2 H_{12}^2 (1+\alpha)^2 \left(\int_0^1 u_k u_l d\bar{x} \right) \quad (21)$$

In the above, $u_k = \frac{2H_2}{CC} \gamma_k$, $u_l = \frac{2H_2}{CC} \gamma_l$ and $w_i' = \frac{\partial w_i}{\partial x}$.

$ff = (l + h_r)^2$ Where $x = l$

$= h_r^2$, where $x = 0$

$= \frac{l^2}{3} + h_r^2 + h_r l$, for other cases.

$[K_{21}]$ is the transpose of $[K_{12}]^T$

The equations (14) and (15) are further simplified to

$$[m]\{\ddot{Q}_{11}\} + [[k] - \bar{P}_0[H]]\{Q_{11}\} - \bar{P}_1 COS(\bar{\omega}\bar{t})[H]\{Q_{11}\} = \{0\} \quad (22)$$

$$[kk] = [K_{12}][K_{22}]^{-1}[K_{12}]^T$$

Where, $[k] = [\bar{k}] - [kk]$ (23)

$$H_{ij} = \int_0^1 w_i' w_j' d\bar{x} \quad (24)$$

2.4. Parametric Instability

Mentioning [42] below expression were written,

$$\ddot{U}_N + \omega_N^{*2} U_N + 2\varepsilon COS\bar{\omega}\bar{t} \sum_{M=1}^{M=p} b_{NM} U_M = 0$$

Where a value of N varies from 1, 2… P.

Where b_{NM} are the matrix's components $[B]$, ω^*_N are the system's distinct Eigen values $\varepsilon = \frac{\bar{P}_1}{2} < 1$ and $[B] = -[Z]^{-1}[M]^{-1}[H][Z]$, where Z denotes the modal matrix $[M]^{-1}[[k] - \bar{P}_0[H]]$

So $\{Q_1\} = [Z]\{U\}$, $\{U\}$ new set of system's generalized coordinates. As a result, the following usages are $\omega^*_{N1} = \omega_{N1,R} + j\omega_{N1,I}$ and $b_{NM1} = b_{NM1,R} + jb_{NM1,I}$ where $\mu = 1, 2, 3 \ldots\ldots N1$

The criteria established by Saito-Otomi [42] are used to delineate the regions of parametric instability in this setup.

3. Results and Discussion

3.1. Comparison and validation

Table 2 Notation Used

Mode	Core-loss factor	Ray, K., and R. C. Kar [27]	Present Analysis	Errors
1	0.18	20	21	+1
	0.6	20.1	21.1	+1
2	0.18	79	79.5	+0.5
	0.6	79.05	79.1	+0.05
3	0.18	178	178.2	+0.2
	0.6	178.02	178.03	+0.01

Table 1 compares the regions of instability for simple resonance obtained from the study by Ray and Kar [27] with the results generated using the present MATLAB code. To align the present analysis with their work, the same parameter values were used. The table demonstrates a strong agreement between the resonance frequencies calculated by Ray and Kar and

International Research Journal on Advanced Engineering and Management
https://goldncloudpublications.com
https://doi.org/10.47392/IRJAEM.2025.0385
e ISSN: 2584-2854
Volume: 03
Issue:07 July 2025
Page No: 2441 - 2450

those obtained in the present study up to the third mode for various core-loss factors. The close match in results validates the accuracy of the current computational approach.

3.2. Dynamic Graphs

Dynamic stability graphs are made for different parameter where the horizontal axis represents for excitation frequency of various parametric value and vertical axis represents the externally applied load (P2). (Figure 2)

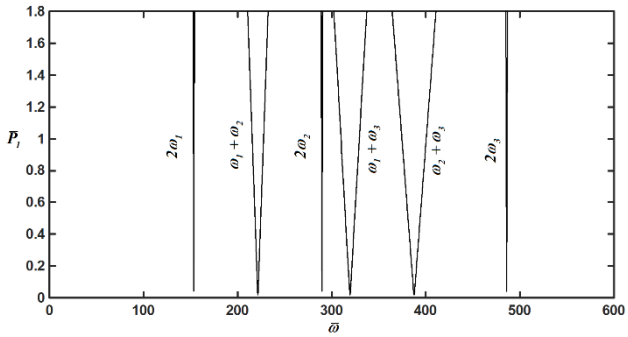

Figure 2 System Stability for (α_1)=0.5

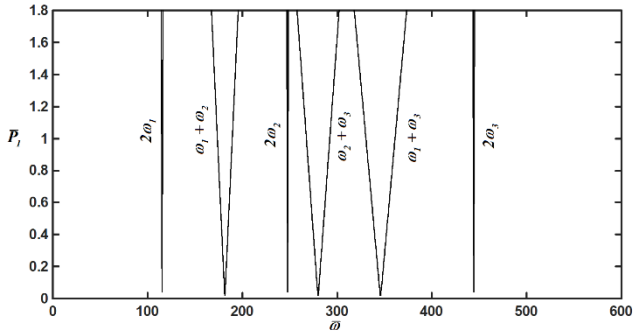

Figure 3 System Stability for (α_1)=0.9

Figures 2 and 3 illustrate the influence of the taper parameter of the upper face layer on the parametric instability zone. As the taper parameter increases, the instability zone gradually shifts towards lower parameter values, indicating a reduction in the system's stability. This increase in the taper parameter corresponds to a higher slenderness ratio and a reduction in mass inertia. Consequently, both the stiffness and the overall rigidity of the system decline. The combined effect of reduced mass inertia and rigidity leads to increased lateral deflection. Therefore, it can be inferred that an increase in the taper parameter adversely affects the stability.

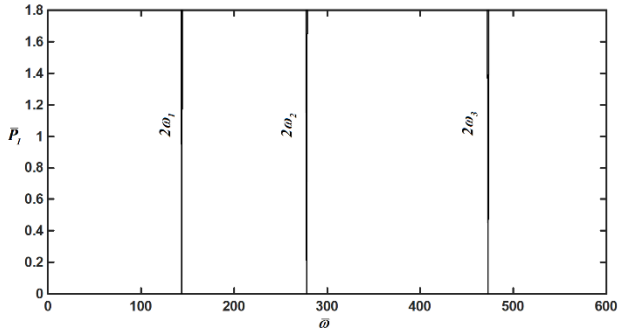

Figure 4 System Stability for (G_s / E)=0.4

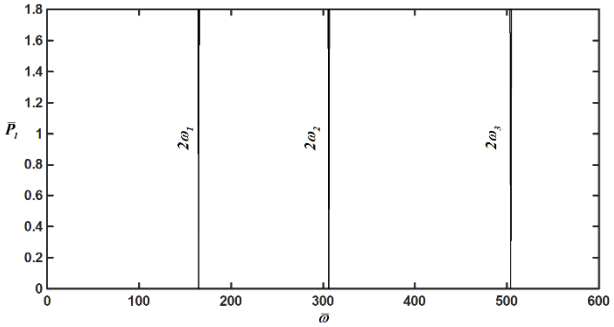

Figure 5 System Stability for (G_s / E)=0.8

Shear parameter's effect on the parametric instability zone can be seen in Figures 4 and 5. A comparison of these numbers shows that by moving instability zone to a upper parametric, value, with increase in shear parameter improves the system's stability. Combination resonance is seen to increase in addition to simple resonance, which causes the instability zone to contract.

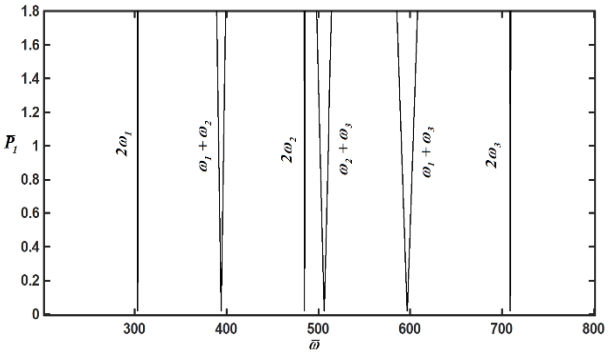

Figure 6 System Stability for (Ω)=9

International Research Journal on Advanced Engineering and Management
https://goldncloudpublications.com
https://doi.org/10.47392/IRJAEM.2025.0385
e ISSN: 2584-2854
Volume: 03
Issue:07 July 2025
Page No: 2441 - 2450

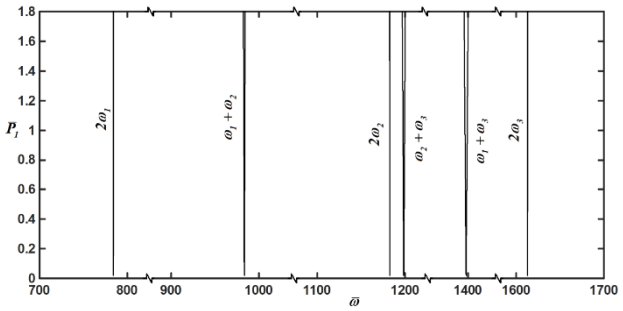

Figure 7 System Stability for (Ω)=15

Figures 6 and 7 illustrate the impact of rotation speed Ω on the parametric instability zone. A comparison of these numbers shows that by moving the instability zone to a higher parameter value, an improve in rotation speed improves the system's dynamic stability. Apart from basic resonance, combination resonance is observed

$$(\omega_1+\omega_2),(\omega_1+\omega_3),(\omega_2+\omega_3),$$

which contributes to a reduction in the parametric instability zones.

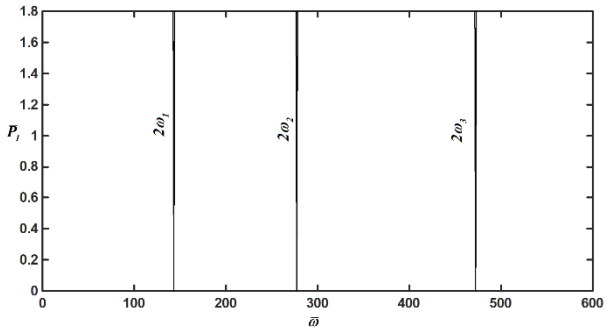

Figure 8 System Stability for (η)=0.5

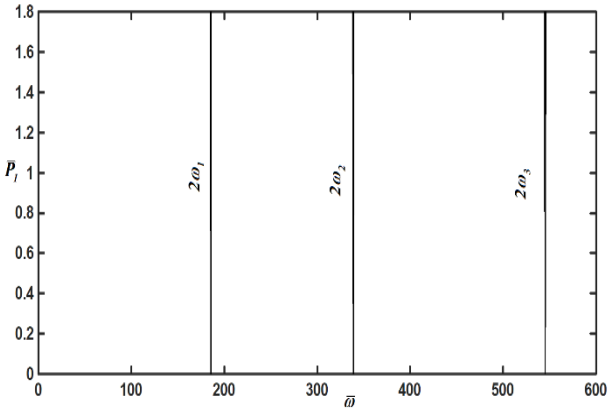

Figure 9 System Stability for (η)=0.8

Figures 8 and 9 depict how the core-loss factor influences the system's dynamic instability. As the core-loss factor increases, it introduces greater energy dissipation (damping) into the system. This added damping suppresses the vibration amplitudes, leading to a noticeable improvement in system stability. As a result, the unstable regions in the parameter space shift upward, indicating that higher values of the excitation or system parameters are now required to induce instability. Thus, the increase in core-loss factor effectively enhances the system's resistance to parametric instability.

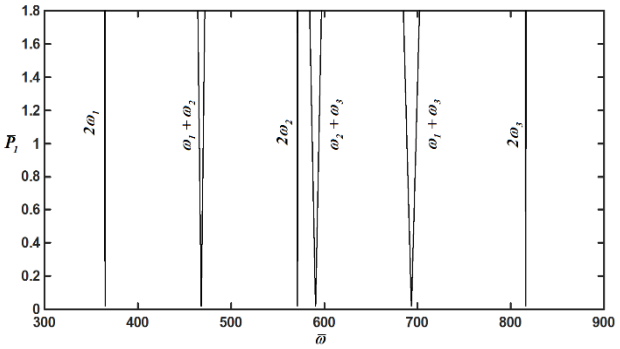

Figure 10 System Stability for (δ_{11})=0.5

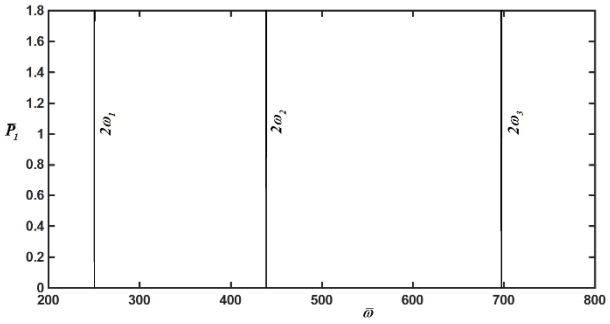

Figure 11 System Stability for (δ_{11})=0.7

Figures 10 and 11 illustrate the effect of the temperature parameter on the system's dynamic stability. A comparison of these figures reveals that increasing the temperature gradient shifts the instability zones toward lower parameter values, indicating a reduction in overall system stability. This behavior can be attributed to the influence of the thermal gradient on the tapered beam, which alters the material properties along its length. Specifically, as the temperature increases, the modulus of elasticity

International Research Journal on Advanced Engineering and Management
https://goldncloudpublications.com
https://doi.org/10.47392/IRJAEM.2025.0385
e ISSN: 2584-2854
Volume: 03
Issue:07 July 2025
Page No: 2441 - 2450

decreases, leading to a significant reduction in the beam's stiffness and rigidity. This weakening of structural rigidity increases the system's susceptibility to dynamic deflections. Additionally, the presence of a temperature gradient can induce non-uniform thermal stresses, further destabilizing the system. Both simple and combination resonances are observed in the response, with the latter becoming more pronounced at higher temperature parameters. Overall, the results clearly demonstrate that an increase in the temperature parameter has a destabilizing effect on the system.

Conclusion

This study has presented a comprehensive analytical and numerical investigation into the dynamic stability of sinusoidally tapered rotating sandwich beams subjected to combined periodic axial loads and thermal gradients. By employing extended Hamilton's principle and the generalized Galerkin method, the governing non-dimensional equations were derived and solved to identify regions of parametric instability.The results reveal that the sinusoidal taper significantly affects the stability boundaries by altering the mass distribution and stiffness characteristics of the beam. Increasing the taper parameter of the upper face sheet reduces the system's rigidity and mass inertia, leading to a shift in the instability zones toward lower excitation parameters, thereby decreasing stability. Similarly, rising temperature gradients reduce the modulus of elasticity, weakening the structure and increasing its susceptibility to instability. On the other hand, the inclusion of core-loss damping enhances system stability by suppressing vibrational amplitudes and pushing instability regions to higher parameter values. Additionally, increasing rotational speed contributes positively to stability, while combination resonances observed throughout highlight the nonlinear interactions within the system.Overall, the study provides valuable insights for optimizing the design of rotating beam structures in thermally and dynamically demanding environments, such as those found in aerospace and energy applications. Future work could extend the analysis to include experimental validation and nonlinear geometric effects for further design optimization.

Acknowledgements

The authors gratefully acknowledge the financial support received from the Department of Science and Technology, Government of Odisha, under Grant No. 175/ST, dated 12.01.2024, which made this research possible.

References

[1]. Faraday, M., "On a peculiar class of acoustical figures and on certain forms assumed by a group of particles upon vibrating elastic surfaces", Phil. Trans., Roy. Soc., 299-318 (1831)

[2]. Hetenyi, M., "Beams of Elastic Foundation", Michigan, The University of Michigan Press, 1946.

[3]. Pradhan, M., & Dash, P. R. (2016). Stability of an asymmetric tapered sandwich beam resting on a variable Pasternak foundation subjected to a pulsating axial load with thermal gradient. Composite Structures, 140, 816-834.

[4]. Yokoyama, T. (1988). Parametric instability of Timoshenko beams resting on an elastic foundation. Computers & structures, 28(2), 207-216.

[5]. Ding, H., Chen, L. Q., & Yang, S. P. (2012). Convergence of Galerkin truncation for dynamic response of finite beams on nonlinear foundations under a moving load. Journal of Sound and Vibration, 331(10), 2426-2442.

[6]. Lenci, S., & Clementi, F. (2012). Effects of shear stiffness, rotatory and axial inertia, and interface stiffness on free vibrations of a two-layer beam. Journal of sound and vibration, 331(24), 5247-5267.

[7]. Pradhan, S. C., &Murmu, T. (2009). Thermo-mechanical vibration of FGM sandwich beam under variable elastic foundations using differential quadrature method. Journal of Sound and Vibration, 321(1-2), 342-362.

[8]. Lenci, S., Clementi, F., & Warminski, J. (2015). Nonlinear free dynamics of a two-layer composite beam with different boundary conditions. Meccanica, 50(3), 675-688.

International Research Journal on Advanced Engineering and Management
https://goldncloudpublications.com
https://doi.org/10.47392/IRJAEM.2025.0385
e ISSN: 2584-2854
Volume: 03
Issue:07 July 2025
Page No: 2441 - 2450

[9]. Chand, R. R., Behera, P. K., Pradhan, M., & Dash, P. R. (2019). Parametric stability analysis of a parabolic-tapered rotating beam under variable temperature grade. Journal of Vibration Engineering & Technologies, 7(1), 23-31.
[10]. Pradhan, M., Dash, P. R., Mishra, M. K., & Pradhan, P. K. (2019). Stability analysis of a tapered symmetric sandwich beam resting on a variable Pasternak foundation. International Journal of Acoustics & Vibration, 24(2).
[11]. Hetényi, M., &Hetbenyi, M. I. (1946). Beams on elastic foundation: theory with applications in the fields of civil and mechanical engineering (Vol. 16). Ann Arbor, MI: University of Michigan press.
[12]. Clementi, F., Demeio, L., Mazzilli, C. E. N., & Lenci, S. (2015). Nonlinear vibrations of non-uniform beams by the MTS asymptotic expansion method. Continuum Mechanics and Thermodynamics, 27(4), 703-717.
[13]. Chonan, S. (1982). Vibration and stability of sandwich beams with elastic bonding. Journal of sound and vibration, 85(4), 525-537.
[14]. Chonan, S. (1982). Vibration and stability of a two-layered beam with imperfect bonding. The Journal of the Acoustical Society of America, 72(1), 208-213.
[15]. Asnani, N. T., &Nakra, B. C. (1970). Vibration analysis of multilayered beams with alternate elastic and viscoelastic layers. Journal of Institution of Engineers India, Mechanical Engineering Division, 50, 187-193.
[16]. Asnani, N. T., &Nakra, B. C. (1976). Vibration damping characteristics of multilayered beams with constrained viscoelastic layers.
[17]. Asnani, N. T. (1996). Vibrations of Damped Multilayered Structures. In Proceeding of Indo-US Symposium on Emerging Trends in Vibration and Noise Engineering (pp. 209-215).
[18]. Pradhan, M., Dash, P. R., & Pradhan, P. K. (2016). Static and dynamic stability analysis of an asymmetric sandwich beam resting on a variable Pasternak foundation subjected to thermal gradient. Meccanica, 51(3), 725-739.
[19]. Hetényi, M., &Hetbenyi, M. I. (1946). Beams on elastic foundation: theory with applications in the fields of civil and mechanical engineering (Vol. 16). Ann Arbor, MI: University of Michigan press.
[20]. Kerwin Jr, E. M. (1959). Damping of flexural waves by a constrained viscoelastic layer. The Journal of the Acoustical society of America, 31(7), 952-962.
[21]. Wang, T. M., & Stephens, J. E. (1977). Natural frequencies of Timoshenko beams on Pasternak foundations. Journal of Sound Vibration, 51(2), 149-155.
[22]. Clementi, F., Demeio, L., Mazzilli, C. E. N., & Lenci, S. (2015). Nonlinear vibrations of non-uniform beams by the MTS asymptotic expansion method. Continuum Mechanics and Thermodynamics, 27(4), 703-717.
[23]. Caruntu, D. I. (2008, January). On nonlinear forced response of nonuniform beams. In Dynamic Systems and Control Conference (Vol. 43352, pp. 403-408).
[24]. Yu, Y. Y. (1962). Nonlinear flexural vibrations of sandwich plates. The Journal of the Acoustical Society of America, 34(9A), 1176-1183.
[25]. Sorge, F. (1995). On the flexural vibrations of sandwich plates. Meccanica, 30(4), 397-403.
[26]. Sokolinsky, V. S., Von Bremen, H. F., Lavoie, J. A., & Nutt, S. R. (2004). Analytical and experimental study of free vibration response of soft-core sandwich beams. Journal of Sandwich Structures & Materials, 6(3), 239-261.
[27]. Ray, K., and R. C. Kar. "Parametric instability of a sandwich beam under various boundary conditions." Computers & structures 55.5 (1995): 857-870.
[28]. Howson, W. P., &Zare, A. (2005). Exact dynamic stiffness matrix for flexural vibration of three-layered sandwich beams. Journal of Sound and Vibration, 282(3-5), 753-767.
[29]. Chakrabarti, A., &Bera, R. K. (2006). Large

International Research Journal on Advanced Engineering and Management
https://goldncloudpublications.com
https://doi.org/10.47392/IRJAEM.2025.0385
e ISSN: 2584-2854
Volume: 03
Issue:07 July 2025
Page No: 2441 - 2450

amplitude vibration of thin homogeneous heated orthotropic sandwich elliptic plates. Journal of Thermal Stresses, 29(1), 21-36.
[30]. Szekrényes, A. (2015). A special case of parametrically excited systems: free vibration of delaminated composite beams. European Journal of Mechanics-A/Solids, 49, 82-105.
[31]. Wang, Y. H., Tham, L. G., & Cheung, Y. K. (2005). Beams and plates on elastic foundations: a review. Progress in Structural Engineering and Materials, 7(4), 174-182.
[32]. Cheng, F. Y., &Pantelides, C. P. (1988). Dynamic Timoshenko beam-columns on elastic media. Journal of Structural Engineering, 114(7), 1524-1550.
[33]. Lenci, S., & Clementi, F. (2012). Effects of shear stiffness, rotatory and axial inertia, and interface stiffness on free vibrations of a two-layer beam. Journal of sound and vibration, 331(24), 5247-5267.
[34]. Gibson, R. F. (2010). A review of recent research on mechanics of multifunctional composite materials and structures. Composite structures, 92(12), 2793-2810.
[35]. Girhammar, U. A., & Pan, D. (1993). Dynamic analysis of composite members with interlayer slip. International Journal of Solids and Structures, 30(6), 797-823.
[36]. Clementi, F., Demeio, L., Mazzilli, C. E. N., & Lenci, S. (2015). Nonlinear vibrations of non-uniform beams by the MTS asymptotic expansion method. Continuum Mechanics and Thermodynamics, 27(4), 703-717.
[37]. Sato, M., Kanie, S., &Mikami, T. (2008). Mathematical analogy of a beam on elastic supports as a beam on elastic foundation. Applied Mathematical Modelling, 32(5), 688-699.
[38]. Ding, H., Chen, L. Q., & Yang, S. P. (2012). Convergence of Galerkin truncation for dynamic response of finite beams on nonlinear foundations under a moving load. Journal of Sound and Vibration, 331(10), 2426-2442.
[39]. Babilio, E. (2013). Dynamics of an axially functionally graded beam under axial load. The European Physical Journal Special Topics, 222(7), 1519-1539.
[40]. Koizumi, M. F. G. M. (1997). FGM activities in Japan. Composites Part B: Engineering, 28(1-2), 1-4.
[41]. Filiz, S., &Aydogdu, M. (2015). Wave propagation analysis of embedded (coupled) functionally graded nanotubes conveying fluid. Composite Structures, 132, 1260-1273.
[42]. Wang, L., Ma, J., Peng, J., & Li, L. (2013). Large amplitude vibration and parametric instability of inextensional beams on the elastic foundation. International Journal of Mechanical Sciences, 67, 1-9.
[43]. H. Saito and K. Otomi, “Parametric response of viscoelastically supported beams”. Journal of Sound and Vibration, 1979, 63, 169-178.
[44]. Ray, K., and R. C. Kar. "Parametric instability of a sandwich beam under various boundary conditions." Computers & structures 55.5 (1995): 857-870.